Biological and Applied Sciences

Vol.60: e17160511, January-December 2017
http://dx.doi.org/10.1590/1678-4324-2017160511
ISSN 1678-4324 Online Edition

BRAZILIAN ARCHIVES OF BIOLOGY AND TECHNOLOGY

A N I N T E R N A T I O N A L J O U R N A L

Using Bio-Replicated Forming Technologies to Fabricate Shark-Skin Surface

Xia Pu [1,2], Guangji Li [1*], Hanlu Huang [2], Yunhong Liu [1], Muhammad Aqeel Ashraf[3].

[1] School of Materials Science and Engineering, South China University of Technology, Guangzhou 510640, China; [2] College of Chemistry & Chemical Engineering, Zhongkai University of Agriculture and Engineering, Guangzhou 510225, China; [3] Faculty of Science and Natural Resources, University Malaysia Sabah 88400 Kota Kinabalu, Sabah, Malaysia.

ABSTRACT

Shark-skin surfaces show the non-smoothness characteristics due to the presence of riblet structures. In this work, biomimetic shark-skins were prepared by means of different bio-replicated forming techniques. These techniques include the PDMS elastomeric stamping method (e.g., PES method) and the PDMS embedded-elastomeric stamping method (e.g., PEES method). The study characterized the fabricated biomimetic surfaces through the use of scanning electron microscopy (SEM) as well as 3D microscope. The accuracy of the two replication routes were compared, which included measuring the surface integrity and dimensional parameters (s, h) of the riblet-groove structure. The results show that fresh shark-skin without chemical treatments should be used as a replication template whenever possible to attain a satisfactory replication accuracy of the riblet structure. The PES and PEES methods proposed here are effective bio-replicated forming routes in simulating the microstructures of a shark-skin surface. Compared with the PES method, the PEES method has greater precision in simulating the microstructures of a shark-skin surface.

Key words: shark skin, micro-structured, bio-replicated forming technologies, embedded-elastomeric stamping, replication accuracy.

[*]Author for correspondence: pu_xia@126.com

INTRODUCTION

Bionics refers to biologically inspired design that has been adapted or derived from nature. Bionics is defined as “the study of the formation, structure or function of biologically produced substances and materials and biological mechanisms and processes especially for the purpose of synthesising similar products by artificial mechanisms which mimic natural ones” [Bhushan 2009]. In practice, bionics is a highly interdisciplinary field of science that includes chemistry, physics, biology, physical chemistry, optics, mechanics, and many other fields. In recent years, considerable progress has been made in designing and manufacturing nanomaterial, nanodevices, functional surfaces, etc. by mimicking biology and nature. A good example of this type of bionic design is the biomimetic drag reduction that is achieved using a special microstructure surface that emulates the non-smooth surface of certain natural species. Biomimetic drag reduction saves energy and is environmentally friendly because no additional energy is required and no chemicals are released in the drag reduction process. With hopes of further improving drag reduction, the microstructures on the surface of the skin of fast-swimming sharks have been observed and analysed. Shark-skin is covered by tiny individual tooth-like scales called dermal denticles, which are ribbed with longitudinal grooves that are aligned in the streamwise direction. This design results in a non-smooth shark-skin surface that appears as an intriguing three-dimensional (3D) riblet pattern [Reif 1985]. Inspection of the shark-skin surfaces for different shark species reveals variations in the detailed riblet or groove structure in the shark scales among species [Reif 1978] and with the location of riblets on the skin of a given species of shark [Reif 1985]. The dermal denticles on a shark-skin surface form an interlocking array [Reif 1985].

In order to clarify the effects of shark-skin's non-smooth surface in relation to reducing drag, some biomimetic surfaces with similar microstructures have been designed and manufactured [Bechert et al 1997, Bhushan et al 2012, Li et al, 2014]. These manufactured surfaces were then evaluated in terms of their drag reduction capability [Walsh 1982, Walsh 1984, Elfriede et al 2010]. The investigated biomimetic surfaces had riblet structures with cross-sectional designs that included a sawtooth, scallops, a blade, and other shapes. Compared with a flat surface that served as a control specimen, these biomimetic surfaces reduced the drag in fluid flow by 5% to 10% [Walsh 1984, Bhushan et al 2012]. The drag reduction mechanism of riblets has been explored by numerical turbulent flow simulations and experiments on fluid flow over riblet surfaces [Golstein et al 1995, Elfriede et al 2010, Amy et al 2014]. The results from these experiments indicated that riblet structures can hinder the translation of the streamwise vortices and lift the vortices off the respective surface, which reduces the outer-layer turbulence and the surface area that is exposed to the high-velocity flow, respectively [Walsh 1982, Amy et al 2014]. Thus, the velocity distribution or fluctuations are modified, resulting in a net drag reduction. These studies prove that a non-smooth shark-skin surface with special microstructures is an excellent natural template for a low-drag surface. This design has motivated many attempts to fabricate biomimetic surfaces by simulating the microstructures and riblet structures of shark-skin surfaces and studying the associated drag reduction.

The fabrication of a biomimetic shark-skin surface is a prerequisite to studying the effect of the shark-skin on drag reduction; thus, different routes for fabricating these surfaces have been explored for decades. These routes can be broadly divided into three categories in terms to the characteristic processing features. The first two routes use direct and indirect methods for manufacturing the surface microstructures, and the third route uses a bio-replicated forming method. A real shark-skin is not required as an original template for either the direct or indirect manufacturing methods. The riblet

structures and the negative riblet contours are constructed on the surfaces of various substrates by abstracting and then simplifying the microscopic shape of real dermal denticles. This procedure produces a biomimetic surface and a negative mould for preparing this surface. Typical substrates are polymers, metals, and crystalline silicon. Feasible techniques for constructing surface microstructures include surface scratching [Weiss 1997], surface machining [Walsh 1984], diamond fly cutting processing [Zhao 2009], photolithography [James et al 2007], laser etching [Gregory and Bhushan 2013, Xu et al 2014], grinding [Denkena 2010], and rolling [Hirt and Thome 2008]. These techniques offer the advantage of being easy to adapt for producing riblet geometries and cross-sectional shapes. However, these techniques have the disadvantage that the fabricate surfaces are relatively dissimilar to a real shark-skin, which exhibits a rather intriguing 3D interlocking riblet pattern. These techniques also often require special equipment and involve a complicated manufacturing process, which lowers the efficiency of the methods. In contrast, the bio-replicated forming method is a facile and effective route to fabricating a biomimetic surface that appears very similar to a real shark-skin. This method involves the micro-replication of surface microstructures using a real biological surface, such as a shark-skin surface, as the original template. Two specific technical applications of this method include micro-moulding and micro-embossing, in which chemically treated shark-skin is used as a template and a rigid plastic, polymethylmethacrylate (PMMA), is used as the matrix of a negative mould [Han and Zhang 2008]. The fabricated biomimetic shark-skin possesses a relatively accurate shark-skin surface morphology. However, the demoulding process can be difficult and often damages the surface microstructures because of a decrease in the flexibility and elasticity of the moulded material. Therefore, these micro-replication methods can be improved further.

The elastic matrix of a non-smooth shark-skin is similar to that of the smooth skin of a dolphin and may reduce drag because of its excellent transition-delaying properties [Carpenter and Garrad 1986]. In the bio-replicated forming method, polymeric materials can be used as highly elastic substrates because of their excellent processability, ease of moulding and demoulding, and a wide spectrum of other physical and mechanical properties. We considered that a biomimetic surface possessing both the surface microstructures and matrix characteristics of real shark-skin could be fabricated by improving the production technique. We selected the cross-linkable elastomer polydimethylsiloxane (PDMS), which has excellent flexibility, low energy, and ease of moulding, as the mould material to replicate the microstructures that were reported in our previous study [Su et al 2008]. This technique is called the PDMS elastic stamping (PES) method and involved the concept of soft lithography. Research results indicated that this technique results in easy demoulding and a high-quality surface. However, the shrinkage and inferior permeability of the PDMS elastomer have detrimental side effects on the replication accuracy. Zhao et al. laid multilayer glass fibres to reduce the shrinkage of PDMS; however, the glass fibres that were used in this process can have a significantly detrimental effect on the PDMS fluidity and the quality of the surface [Zhao et al 2012].

In this study, we developed an efficient method of fabricating surface microstructures based on the PES method. We used a critical step of embedded embossing to develop the PDMS embedded elastomeric stamping (PEES) method to prepare the negative mould. A prerequisite to performing this technique is the preparation of shark-skins with excellent flexibility without the application of chemicals. Therefore, we also developed a novel non-chemical shark-skin treatment in this study. PDMS and polyurethane (PU) elastomers were used as substrates for the negative mould and the

biomimetic shark-skin surface, respectively. 3D scanning and scanning electron microscopy (SEM) were used to observe the surface morphology and the riblet geometries of the biomimetic shark-skin and the shark-skin templates. We evaluated the replication accuracy of the two fabrication techniques in terms of the surface integrity, the dimensional parameters, and the cross-sectional contours of the riblet-groove structures.

EXPERIMENTAL

Materials and reagents

Fresh shark-skin from one of the fastest swimming sharks, the great white shark (Carcharodon carcharias), was purchased from a fisherman. A two-component room temperature vulcanisable liquid silicone rubber, including a low-velocity precursor of vinyl-PDMS and a curing agent, was obtained from Zhejiang Runhe Silicone New Material Co., Ltd. The PDMS contained 25% of fumed silica (300 m^2/g) filler, which was treated with $Si(Me)_2$-O-oligomers. A two-component room temperature vulcanisable liquid polyurethane, including a precursor and curing agent, was used to fabricate a biomimetic shark-skin surface. The precursor with a 4.8% isocyanate (NCO) content was obtained by reacting diisocyanate with polytetramethylene ether glycol. The formaldehyde, alcohol, and acetone reagents were all analytical grade.

Pretreatment of fresh shark-skin

First, the subcutaneous fat from the fresh shark-skin was removed. The shark-skin was then washed several times with deionised water and cut into the required shape. Several sheets of fresh shark-skin were cut out from symmetrical anterior positions of the shark's body. Some of these samples were left out for the subsequent replication procedure, and the remaining samples were stored in a refrigerator before use. A non-chemical treatment method was designed to preserve the original elasticity, ductility, and surface integrity of the shark-skin. Several chemical treatments were also employed for comparison purposes.

The non-chemical treatment process is described below. Several sheets of fresh skin were fixed onto plates, or clamped between two glass plates, and oven-dried at 40-60°C for 1 to 2 h to produce semi-dried skins with moisture contents of approximately 20%. These semi-dried skins were labelled FSR. To prevent the skins from shrinking and warping, a mixture of the PDMS precursor and a curing agent (10:1 by weight), which served as an elastic matrix, was layered at a thickness of approximately 1 mm and flattened on the back of the FSR, which was then cured at room temperature for 2-3 h. The FSR that was processed with the cured PDMS elastic matrix was labelled P-FSR.

The chemical treatment process is described below. Following related references [Han and Zhang 2008, Zhao et al 2012], the fresh shark-skin was treated with 2.5% glutaraldehyde liquor and an aqueous ethanol solution. This chemically treated shark-skin sample was labelled CSR-A. The fresh shark-skin sample was also treated using 10% formalin liquid. This final sample was labelled CSR-B.

Isolation of a single denticle

A small piece of fresh shark-skin was soaked in a Na_2HPO_4 buffer solution (10 mmol/l, pH 7.4-7.6) for 1-2 h, after which the proteins (or collagens) that were attached to the roots of the denticles and that fixed the denticles to the dermis were removed. Tiny tweezers were used to isolate a single denticle from the skin under a XSP-I high-power microscope.

Fabrication of biomimetic surfaces based on shark-skin

The biomimetic surfaces based on shark-skin were fabricated using the PES and PEES methods.

PDMS elastomeric stamping method

The PES process consisted of the following steps. First, a plate with the shark-skin template (FSR) was prepared as a mould for casting, as shown in Fig. 1(a). This mould was labelled Mold-A. Second, a mixture of the PDMS precursor and the curing agent (10:1 by weight) was poured into Mold-A and evacuated in a vacuum oven for 2-10 min. The mixture was allowed to solidify at room temperature for 30 min and was then separated from the mould. This mould was then used to fabricate the desired shark-skin replica (SSR-1) and a PDMS sheet with a contrary-shaped surface profile corresponding to the said shark-skin. Third, the SSR-1 template was used to manufacture a cavity block (or negative mould) by the same process as was described in the first step. This negative mould was labelled Mold-B. Finally, the PU pre-polymer and the curing agent were mixed and degassed in a desiccator, which was then poured into Mold-B. After curing and demolding, the PU sheet with the microstructure of shark-skin surface (S-PU) was completely fabricated.

PDMS embedded elastomeric stamping method

The PEES method is described here. As illustrated in Fig. 1(b), a mixture of the PDMS pre-polymer and the curing agent (10:1 by weight) was first poured into a plate and evacuated in a vacuum oven for 2-10 min. Next, the shark-skin template (P-FSR) with its scale side down was carefully embedded onto the surface of an uncured PDMS sheet. Isostatic pressure, of a magnitude that depended on the template area, was applied to the P-FSR to transfer the surface microstructures of the shark-skin to the PDMS surface in contact with the shark-skin. After curing at room temperature for 30 minutes, the P-FSR was separated from the cured PDMS sheet for micro-replication at which point the shark-skin replica (SSR-2) and PDMS sheet as a negative mold were fabricated. The fabrication procedure for the PU sheet with the microstructure of the shark-skin surface (E-PU) was similar to that of the PES method. A PDMS sheet with a shark-skin surface microstructure (E-PDMS) was fabricated using the same micro-replication process as in the preceding step.

A mixture of the PU pre-polymer and the curing agent was poured into a plate and cured to obtain a flat PU sheet, which was labelled F-PU. A flat PDMS sheet was also prepared using the same method and labelled F-PDMS.

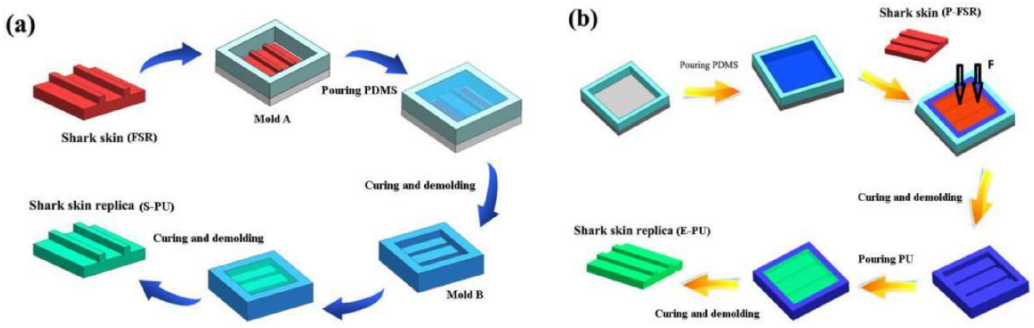

Fig.1. Schematic of micro-replication of shark-skin surface: (a) PDMS elastomeric stamp method (PES method) and (b) PDMS embedded-elastomeric stamp method (PEES method)

Measurement and characterisation

Calculating the shrinkage ratio of a shark-skin sample from chemical treatment
The shrinkage ratio of the shark-skin samples that were produced with a chemical treatment corresponded to the percentage shrinkage of the surface area, which was obtained by comparing the surface area of the chemically treated shark-skin to fresh shark-skin. Before processing the fresh shark-skin, a rectangular region was selected and marked: the area of the region is denoted by A_0 . The area of this region after processing is denoted by A_1. The shrinkage ratio of the chemically treated shark-skin can be expressed as follows:

$$S = \frac{A0 - A1}{} \times 100\%$$

Tensile test of shark-skin

The tensile performance of shark-skin was measured according to ISO37: 2005 using a UT-2080 material testing machine from U-CAN DYNATEX INC, Taiwan, China. The FSR, CSR-A and CSR-B samples were tested using this device.

Surface characterisation
The shark-skin surface morphology and the prepared microstructure sheets were observed using a SEM (S-3700N, Hitachi, Japan) and a XSP-15CC light microscope (Shanghai, China).
The geometries of the microstructure of the biomimetic shark-skin surfaces were evaluated by measuring the replication precision indexes using a Hirox 7700 (Japan) 3D microscope. The microscope was used for the 3D scanning and imaging of the surfaces of the shark-skin replicas and the biomimetic shark-skin sheets with microstructures.

Contact angle measurements
The CA was measured using a contact angle goniometer (DSA 100, Krüss GmbH, Germany) at ambient temperature. Each sample was measured three times at three random locations, and the average of the measured values was reported.

RESULTS AND DISCUSSION

Structure of dermal denticles

The surface morphology of the shark-skin and the geometries of the riblet groove of the dermal denticles were observed using a SEM. As shown in Fig. 2(a), the scale-shaped denticles formed an interlocking arrangement along the long axis of the shark's body, which lay in the direction of motion of the shark. Each denticle showed a typical coronal structure with several riblets and grooves that were arranged in an alternating pattern. As shown in Fig. 2(b) and Fig. 2(c), the estimated size of a denticle was approximately 0.2-0.5 mm (side length), the height of a riblet was approximately 8 μm, and the spacing between two adjacent riblets was approximately 60 μm.

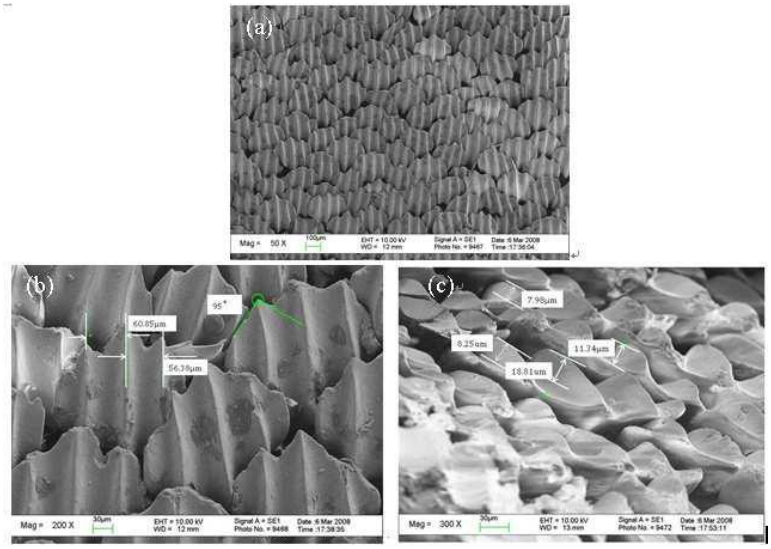

Fig.2. SEM images of riblet structure of shark-skin surface at magnifications of (a) 50×, (b) 200×, and (c) 1000

A single denticle was extracted from the skin, and its stereo shape was observed and recorded (Fig. 3(a) and Fig. 3(b)). The images show that the denticle consisted of a coronal scale consisting of hard enamel and a root or base plate that was deeply embedded in the elastic dermal layer of the shark-skin. This root fixed the denticle to the shark-skin surface, such that the denticle functioned as a cantilever. Variations in the fluid pressure may deform the elastic skin of a swimming shark to a certain extent. This deformation, in turn, produces a corresponding inclination in the hard coronal part of a denticle, which corresponds to the angle between the direction of the riblets and the direction of the water flow. Consequently, there is a reduction in the wall shear stress. Therefore, we attribute the drag reduction by shark-skin to the surface layer of dermal denticles combined with the basal matrix. Fig. 3(c) and Fig. 3(d) show the surface morphologies of the raised ridge and the concave groove of the denticle, respectively. Nanostructured protuberances were found on the surface of the concave groove. However, the surface of the raised ridges was relatively smooth. Using the results of a study on the surface structure of a superhydrophobic lotus leaf [Lin et al 2002], we hypothesise that the nano-roughness of the denticles on the shark-skin surface may effectively prevent marine organisms from attaching to the shark-skin.

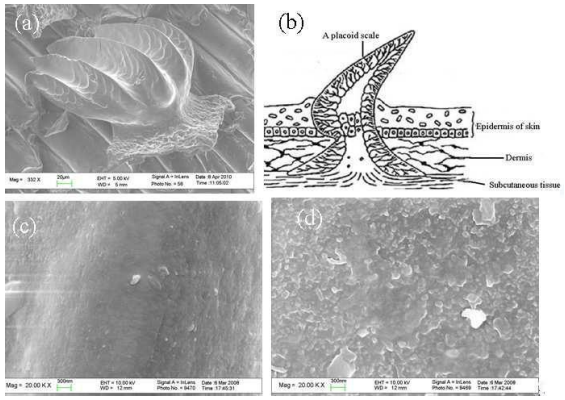

Fig.3. SEM images of single denticle of shark-skin surface: (a) overall structure, (b) model of riblet structure, (c) raised ridge magnified 20000×, and (d) concave groove magnified 20000×

Impact of pretreatment on morphology and mechanical properties of shark-skin

The surface profiles of the chemically treated shark-skin sample (CSR-B) and the fresh shark-skin sample (FSR) are shown in Fig. 4(a) and Fig. 4(b), respectively. These images show that the chemical treatments damaged the shark-skin surface and did not preserve the integrity of the riblet structure. Unlike with the FSR, the scales of the CSR-B developed cracks, and the enamel fell off the edge of the scales, producing an inferior surface topography.

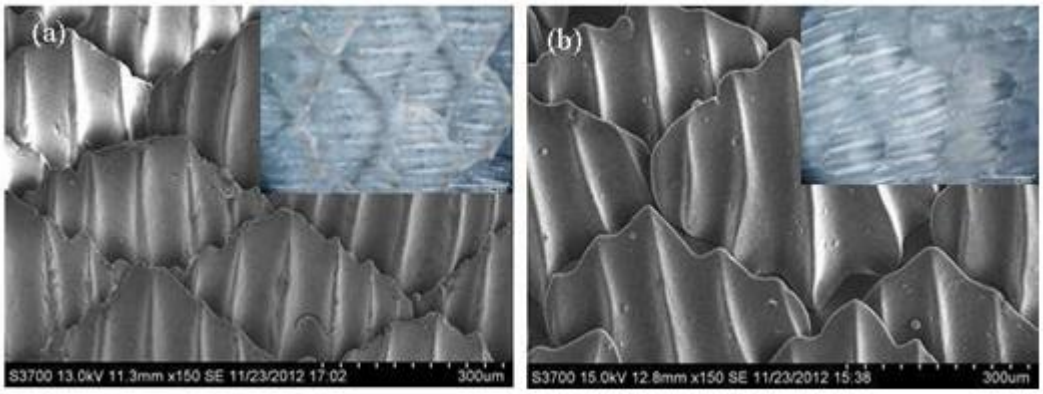

Fig.4. SEM images of shark skin pretreated by different methods: (a) CSR-B and (b) FSR

In addition to this damage, both the CSR-A and CSR-B samples exhibited constrictions from the chemical treatment process and corresponding shrinkages of 10% and 13%, respectively, which resulted in a change in the structure, size, and shape of the riblets. Fig. 5 shows the 3D grooves and the corresponding section profiles that were collected from a single shark scale for the FSR and CSR-B samples. We compared the average groove width *s* and the central spine height *h* (which is given in Table 1) to analyse the changes in the dimensional parameters of the riblet groove structure before and after the chemical treatments. Compared to the dimensions of the FSR sample, the groove width of the CSR-B sample clearly decreased by 1.8% and the central spine height of the CSR-B increased by 17.4%. The architecture of shark-skin, like any other vertebrate skin, consists of an outer epidermis, which overlays a dermis with flesh made up of elastic fibres. Another important characteristic of shark-skin is the waviness of the fibre bundles, which straightens during the tensile testing process. However, the usage of chemical reagents produced disorder in the elastic fibres, thus affecting the mechanical behaviours of the skin specimens. The stress-strain curves of the FSR and CSR-A samples in Fig. 6 suggest that the CSR-A specimen possessed a lower tensile strength and elongation at breaking, as well as a higher modulus and stress at the same elongation as the FSR specimen. Furthermore, the stress-strain curves imply that the FSR sample possessed excellent flexibility and elasticity, whereas the CSR-A sample was strong and tough because of the loss of elasticity, along with the shrinkage of the skin, which resulted primarily from the denaturation of the elastic fibre protein by chemical treatment. The skin shrinkage resulted in an increase in the fibre bundle density per unit area. Thus, the skin became denser and its modulus increased because of the chemical treatment.

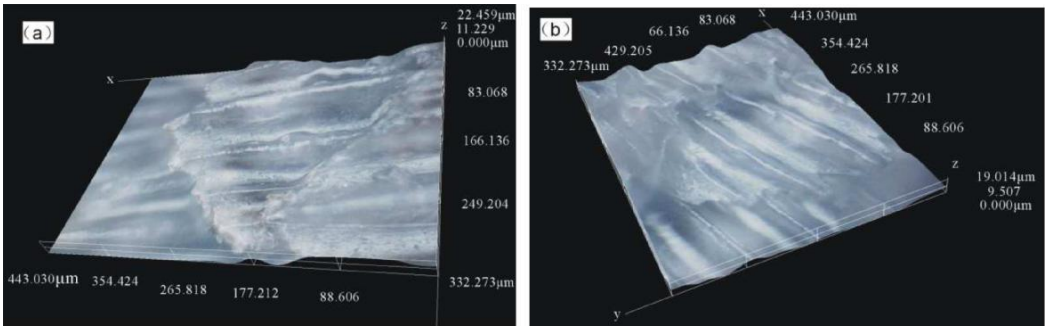

Fig.5. 3D images of single-scale structure: (a) CSR-B and (b) FSR

Table 1 Parametric changes in the riblet dimensions of FSR and CSR-B

Sample	Average groove width s （μm）	Central spine height h （μm）	Deformation ∆s/ s %	Deformation ∆h/ h %
FSR	60.58	9.56	—	—
CSR-B	59.46	11.23	–1.8	+17.4

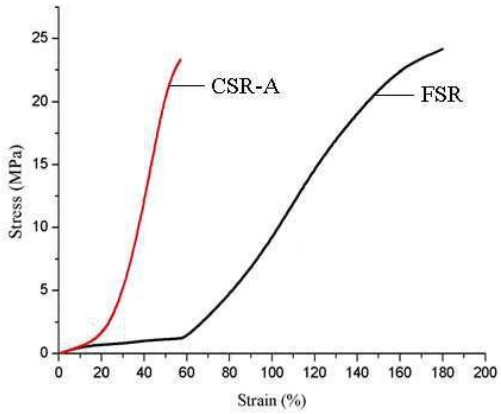

Fig.6. Stress-strain curve for shark-skin

The aforementioned observations show that the FSR without chemical treatment should be used as a replication template to the maximum extent possible to obtain satisfactory replication accuracy for the riblet structure.

Analysis of replication accuracy

The indexes that were used to evaluate the replication accuracy were calculated using the surface integrity, the dimensional parameters (*s*, *h*), and the cross-sectional contour of the riblet groove structure. Fig. 7 shows the morphology of different biomimetic shark-skin surfaces that were prepared using a PU matrix by the PEES and PES methods. The S-PU and E-PU possessed almost the same surface microstructure as that of the dermal denticles on the real shark-skin, which is shown in Fig. 2. The specific properties of the moulding materials, PDMS and PU, played an important role in the replication process. The excellent flow properties of PDMS and PU caused these precursors to fill the interstices of the mould. The subsequent cross-linking process transformed the flowable precursor into a solid sheet, while maintaining conformal contact with the mould cavity to faithfully replicate the fine structure of the mould.

The relatively low surface free energy of PDMS (γ_{sv} = 21.6 dynes/cm^2) [Choi et al 2004] and the elasticity of the cured PDMS and PU enabled the prepared sheet to be easily demoulded. Comparing Fig. 7(b) with Fig. 7(d) clearly shows that the E-PU, which was fabricated by the PEES method, possessed a more well-defined surface topography and a higher integrity than the S-PU. We attributed these enhanced properties to the seepage of a small quantity of pre-polymer liquid underneath the scale spines when the pre-polymer was directly poured onto the shark-skin surfaces in the PES method because the seeped liquid would inevitably have obstructed the demoulding process. However, the amount of pressure that was used in the PEES method ensured that the pre-polymer fully filled in the bottom of the groove.

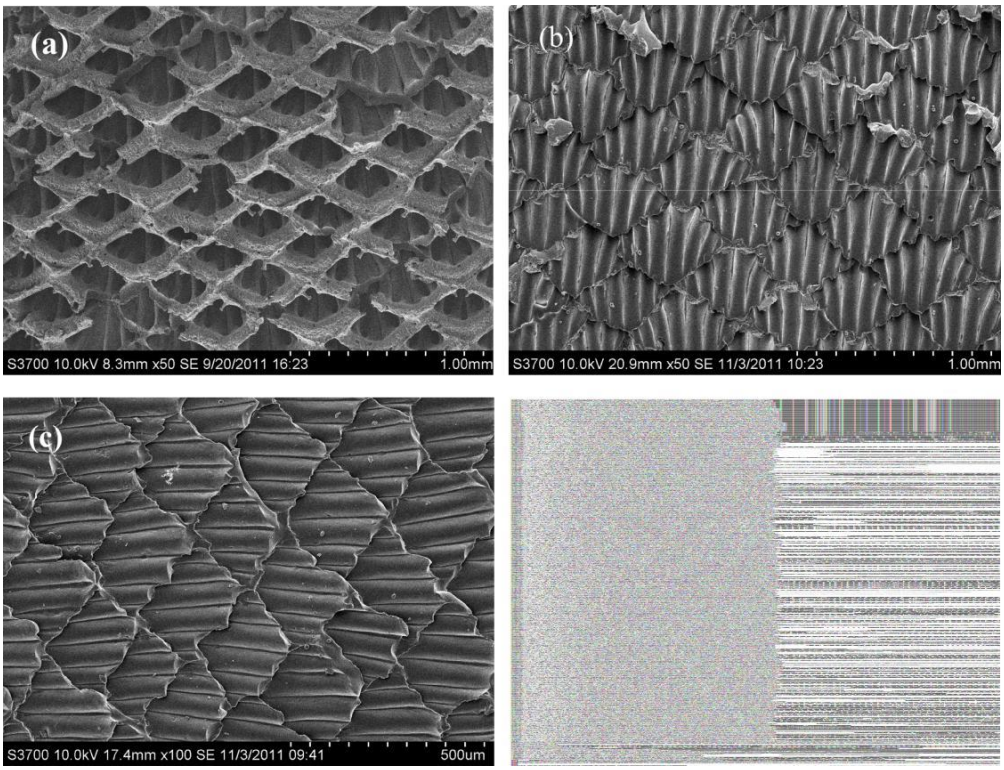

Fig.7. SEM images of surfaces of biomimetic shark-skin prepared via different micro-replication methods: (a) PDMS negative replica prepared by PES method (SSR-1), (b) S-PU, (c) PDMS negative replica prepared by PEES method (SSR-2), and (d) E -PU

A critical step in the PEES method is effective embedded embossing during the preparation of the negative mould. Fig. 8(a) shows the principle of the embedded embossing technique: the P-FSR with excellent flexibility must be used as a template for replication as a prerequisite for this technique. Using our understanding of the shark-skin structure, we first covered the back of the FSR with a sheet of elastic PDMS to serve as a subcutaneous elastic layer (or basal matrix). Only then did we prepare the P-FSR. However, the bending of the P-FSR could have caused a denticle that was embedded in the PDMS elastic layer to bend and deform to a certain extent. This behaviour may have occurred in both the transverse and longitudinal directions of the sample in the elastic embedding process. That is, a denticle may have rotated through a small angle under external pressure, as shown in Fig. 8(b). This phenomenon ensured that the mould pre-polymer fully filled the bottom of the groove.

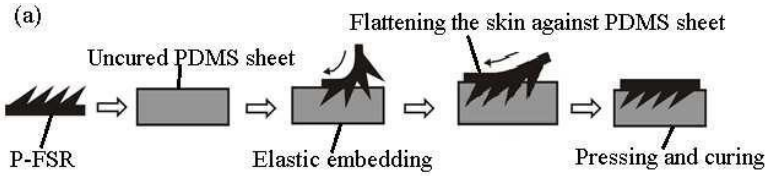

Fig.8. (a) Schematic of operating principle of embedded embossing technique and (b) schematic showing denticle rotation

The key parameters that controlled the replication accuracy of the scale grooves were the groove width "s" and the central spine height "*h*" of the replication templates. Fig. 9 and Fig. 10 show the 3D images and cross-sectional contours of the PDMS negative replicas（SSR-1 and SSR-2）that were prepared by the PEES and PES methods. The average groove width *s* and the central spine height *h* were extracted from these figures and are presented in Table 2. In comparison to the biological samples, the PDMS negative replicas exhibited various deviations in the replication of the riblet structure. Compared with the real shark-skin, the groove widths of the SSR-1 and SSR-2 were higher by 1.96% and 3.2%, respectively, and the heights of the central spines were lower by 8.06% and 2.52%, respectively. These results suggested that there were relatively small errors in the groove dimensions of the SSR-2 replica that was obtained using the PEES method. This result once more indicated that the pressure that was applied in the replication process using the PEES method extended the scale of the groove in the transverse direction, as well as decreasing the shrinkage of PDMS sheet. Therefore, an almost invariable spine height was maintained for the replica that was produced using this method.

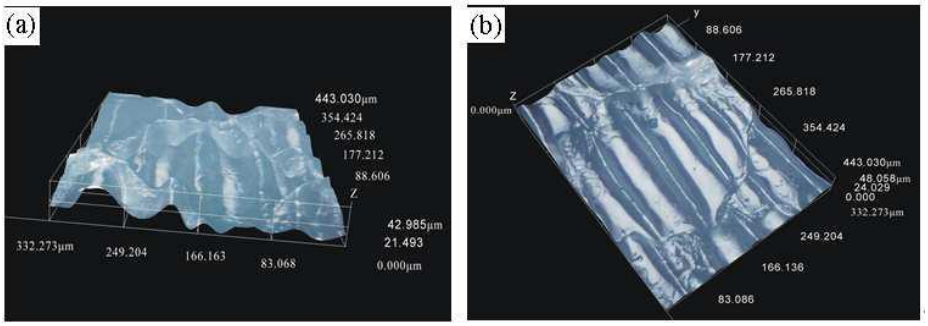

Fig.9. 3D images of a single scale for shark-skin moulds that were prepared using different micro-replication methods: (a) SSR-1 and (b) SSR-2

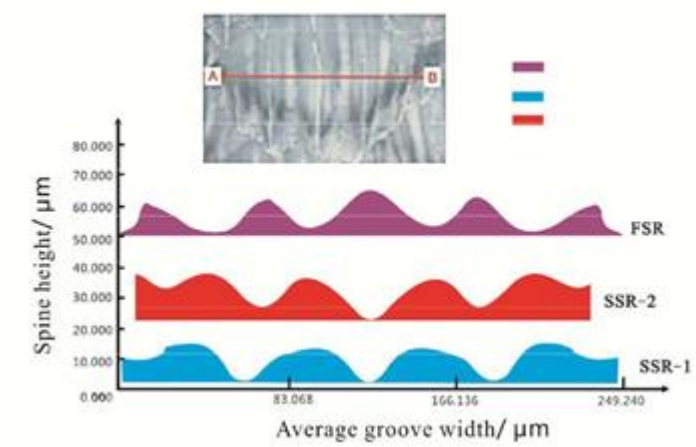

Fig.10. Surface profiles of the real shark skin sample FSR and the negative moulds SSR-1 and SSR-2, which were prepared using the real shark skin sample FSR as a prototype template

Table 2 Comparison of groove dimensions of negative moulds SSR-1 and SSR-2, which were prepared using the real shark skin sample FSR as a prototype template

Sample	Average groove width s （μm）	Central spine height h （μm）	Deformation Δs/ s %	Deformation Δh/ h %
FSR	*60.58*	9.56	-----	-----
SSR-1	63.68	9.12	+1.96	-8.06
SSR-2	64.49	9.43	+3.2	-1.52

Observations of the fine denticle structures on the shark-skin surface revealed nanostructured protuberances on the concave groove surface. Fig. 11 shows the surface profiles of the SSR-1 and SSR-2 samples. These high-magnification SEM images showed that the surfaces of the SSR-1 and SSR-2 were very smooth and did not contain any nanostructured protuberances. Thus, micron-scale surfaces can only be realised using bio-replicated forming techniques.

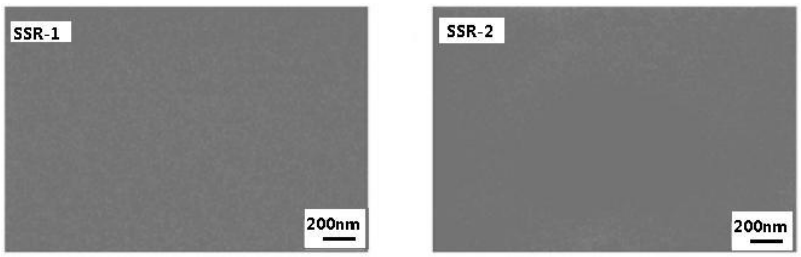

Fig.11. High-magnification SEM images of SSR-1 and SSR-2 surfaces

The comprehensive analysis presented above indicates that the preparation of the negative moulds was critical to the entire replication process. The application of pressure in the preparation of negative moulds created a low surface energy and

ensured high replication accuracy. Therefore, the analysis of the replication precision confirmed that the developed PEES method is an effective bio-replicated forming route to simulate microstructures or riblet structures on shark-skin surfaces.

CONCLUSIONS

Observations on and analyses of a single denticle and fine shark-skin structure revealed that the complete denticle, including the coronal scale and base plate, functioned similarly to a cantilever. Nanostructured protuberances were also found on the concave groove surface. Chemical treatments damaged the shark-skin surface and did not preserve the integrity of the riblet structure. SEM and 3D scanning observations revealed that the biomimetic shark-skins that were prepared using both the PES and PEES methods exhibited well-defined shark-skin surface morphologies or micro-sized shark-skin pattern structures. The shark-skin replica that was prepared using the PEES method also exhibited relatively minor distortions in the groove dimensions because integrating the P-FSR with excellent elasticity as a prototype, PDMS as a negative mould matrix, and the application of pressure in the preparation of the negative moulds.

Although we have made immense progress through studies that have been dedicated to bio-replicated forming methods, the riblet structures in the fabricated biomimetic shark-skin had relatively fixed dimensions and were difficult to change because these structures were fabricated directly on top of the biological samples. Thus, further research on the deformation of biological shark-skin surface morphology is needed. Precisely deformed replicas may be realised by stretching the shark-skin template or negative mould to regulate the scale dimensions and the cross-sectional shapes. In addition, we were not able to capture the fine nanostructured protuberances on the shark-skin surface, and only the micro-structured surfaces could be produced using bio-replicated forming techniques. Therefore, a dual biomimetic surface structure with both a shark-skin surface morphology and lotus-leaf-like hierarchical micro/nano-structures could be created by combining other techniques for fabricating biomimetic surfaces. Finally, further study on the drag reduction and antifouling of the fabricated biomimetic surface is in progress and will be reported in future publications.

ACKNOWLEDGMENTS

This work was financially supported by the National Natural Science Foundation of China (NSFC, Grant No. 50873039). The authors would like to thank Xianyun He and co-workers at the South China University of Technology for generously providing us with a 3D microscope.

REFERENCES

1. Amy W, Michael T, Jonath A, Jennifer N, Philip J. Movable shark scales act as a passive dynamic micro-roughness to control flow separation. Bioinspiration & Biomimetics 2014; 3 : 036017.

2. Bechert D, Bruse M, Hage W, Hoppe G. Experiments on drag reducing surfaces and their optimization with an adjust-able geometry. Journal of Fluid Mechanics 1997; **338:** 59–87.

3. Bhushan B. Biomimetics: lessons from nature–an overview. Philosophical Transactions of the Royal Society of London, Series A 2009; **367:** 1445–86.

4. Carpenter P, Garrad A. The hydrodynamic stability of flow over Kramer-type compliant surfaces Part 2. Flow-induced surface instabilities. Journal of Fluid Mechanics 1986; **170 :** 199–232.

5. Choi S, Yoo P, Baek S, Kim T, Lee H. An ultraviolet-curable mold for sub-100-nm lithography. J Am Chem Soc 2004; 126: 7744.

6. Dean B, Bhushan B. The effect of riblets in rectangular duct flow. Applied Surface Science 2012; 258: 3936–47.

7. Denkena B, Ko¨hler J, Wang B. Manufacturing of functional riblet structures by profile grinding. CIRP Journal of Manufacturing Science and Technology 2010; **3:** 14–26.

8. Elfriede F, Julia P, Thomas R. A study of shark skin and its drag reducing mechanism. Advances in Mathematical Fluid Mechanics 2010; **27:** 1–84.

9. Goldstein D, Handler R, Sirovich L. Direct numerical simulation of turbulent flow over a modeled riblet covered surface. Journal of Fluid Mechanics 1995; **302:** 333–76.

10. Gregory D, Bhushan B. Shark skin inspired low-drag micro-structured surfaces in closed channel flow. Journal of Colloid and Interface Science 2013; **393:** 384–96.

11. Han X, Zhang D. Study on the micro-replication of shark skin. Science in China Series E: Technological Sciences 2008; **55:** 890–96.

12. Hirt G, Thome M. Rolling of functional metallic surface structures. CIRP Annals–Manufacturing Technology 2008; **57:** 317–20.

13. James F, Schumacher, Michelle L, Carman, et al. Engineered antifouling microtopographies-effect of feature size, geometry, and roughness on settlement of zoospores of the green alga Ulva. Biofouling 2007; **23:** 55–62.

14. Lin F, Li S, Li Y, Li H, Zhang L, Zhai J, Song Y, Liu B, Lei J, Zhu D. Super -hydrophobic surfaces: from natural to artificial. Advanced Materials 2002; **14:** 1850–1860.

15. Reif W. Squamation and ecology of sharks. Courier Forschungsinstitut Senckenberg 1985; **78**: 1–255.

16. Reif W, Tйbingen. Types of morphogenesis of the dermal skeleton in fossil sharks. Stuttgart, Juni 1978; **52:** 110–28.

17. Su BH, Li GJ, Pu X, Lei CY. Preliminary study on the replication technology of microstructure of sharkskin on polymer surfaces. Materials Research and Application 2008 **; 4 :** 67–9.

18. Li W, James CW, George VL. Biomimetic shark skin: design, fabrication and hydrodynamic function. The journal of experimental biology 2014; 217: 1656-66.

19. Walsh M. Turbulent boundary layer drag reduction using riblets. AIAA 20th Aerospace Sciences Meeting, Orlando, Florida 1982: 169–76.

20. Walsh M, Lindemann A. Optimization and application of rib lets for turbulent drag reduction. AIAA 22nd Aerospace Sciences Meeting, Reno, Nevada 1984: 347–56.

21. Weiss M. Implementation of drag reduction techniques in natural gas pipelines. In 10th European Drag Reduction Working Meeting, Berlin, Germany, 1997: 19-21 March.

22. Xu J, Zhao W, Peng S, Zeng Z, Zhang X, Wu X, Xue Q. Investigation of the biofouling properties of several algae on different textured chemical modified silicone surfaces. Applied Surface Science 2014; 311: 703-8.

23. Zhao Q, Guo B, Yang H, Wang Y. Technological parameter optimization of micro-structured surfaces by diamond fly-cutting, Optics and Precision Engineering 2009; **17**: 2512–19.

24. Zhao D, Huang Z, Wang M. Vacuum casting replication of micro-riblets on shark skin for drag-reducing applications. Journal of Materials Processing Technology 2012; **212:** 198–202.

Received: February 03, 2016;
Accepted: July 14, 2016